Soft Matter

Accepted Manuscript

This is an *Accepted Manuscript*, which has been through the Royal Society of Chemistry peer review process and has been accepted for publication.

Accepted Manuscripts are published online shortly after acceptance, before technical editing, formatting and proof reading. Using this free service, authors can make their results available to the community, in citable form, before we publish the edited article. We will replace this *Accepted Manuscript* with the edited and formatted *Advance Article* as soon as it is available.

You can find more information about *Accepted Manuscripts* in the Information for Authors.

Please note that technical editing may introduce minor changes to the text and/or graphics, which may alter content. The journal's standard Terms & Conditions and the Ethical guidelines still apply. In no event shall the Royal Society of Chemistry be held responsible for any errors or omissions in this *Accepted Manuscript* or any consequences arising from the use of any information it contains.

ROYAL SOCIETY OF CHEMISTRY

www.rsc.org/softmatter

Please do not adjust margins

Soft Matter

ARTICLE

Gelation Behaviour of a Bent-core Dihydrazide Derivative : Effect of Incubation Temperature in Chloroform and Toluene

Received 00th January 20xx,
Accepted 00th January 20xx

DOI: 10.1039/x0xx00000x
www.rsc.org/

Chunxue Zhang[a], Tianren Zhang[a], Nan Ji[b], Yan, Zhang[a], Binglian Bai[b], Haitao Wang[a], and Min Li[*,a]

In this work, a new kind of gelator, 1,3-bis[(3,4-dioctyloxy phenyl) hydrazide] phenylene (BP8-C), containing two di-hydrazide units as the rigid bent-core, had been synthesized and investigated. It is demonstrated that BP8-C is an efficient gelator which can gel various organic solvents such as ethanol, benzene, toluene and chloroform, etc. Both opaque gel (O-gel) and transparent gel (T-gel) which is more stable, were obtained for BP8-C in chloroform at different incubation temperatures. Kinetic data based on fluorescence sprectra revealed that the T-gels showed a larger Avrami parameter (n = 1.44 at 20 ℃) than that of the O-gels (n = 1.21 for gelation at temperatures below 0 ℃). While BP8-C formed opaque gel in toluene and it took longer time for gelation at lower incubation temperature even precipitated out below 0 ℃. The kinetic Avrami analysis on sols of BP8-C with different concentrations show a two-phrase mechanism, i.e. the n values are between 0.88 to 1.74 followed 1.69 to 3.01 throughout the temperature range of 5 ℃ and 35 ℃ for 5.34 mg/mL BP8-C in toluene, indicating that the fibers formed first and then bundling to produce compact networks. We proposed that the supersaturation govern the formation of gel in chloroform and diffusion process dominant the gelation in toluene. XRD and FT-IR measurement confirmed that the xerogels prepared at different temperatures in different solvents exhibited Col_h structure and there are three molecules in one columnar slice. Our results indicated that gelation process, morphology of the gels and thus final properties of the gels depend strongly on the preparation conditions such as temperature, solvent, concentration etc.

Introduction

Recently, the crystallization-like gelation process enable us a challenging but meaningful nanoengineering method to construct favorable functional material for low molecular mass organogelators (LMOGs), and LMOGs has been a burgeoning field of soft matter science due to its growing number of potential applications in new materials and nanoscale devices[1-3], especially in bioscience[4-6] and bionics[7-10]. Most of the investigations of LMOGs focus on the synthesis of gelators and characterization of the gel behaviour, relatively little is paid on the mechanism of gel formation and the role of solvents on gelation. While there is a general consensus that the self-assembled fibrillar networks form via crystalline nature, i.e., nucleation - growth - rearrangement of the network. Many publications dealed with the influence of factors on the growth of the fiber, such as concentration[11], incubation temperature[12-15], pH[16-17], ultrasound[18-20]and solvents[21-23] and even the steps taken to prepare. As far as the annealing temperature is concerned, the nucleation and fiber growth processes are governed by mass transfer or thermodynamics. For the nucleation stage of crystallization process, classical nucleation theory is widely accepted, in which fluctuations was considered to give rise to the appearance of a small nucleus[24]. Recently, a two-step mechanism was proposed for protein crystallization by Vekilov and co-workers[25], e.g. the liquid-drop formed first caused by microphase separation then the molecules progressively restructure into compact nucleus. Several groups reported the mechanism of nucleation in LMOGs system. In Meijer's work, they found the oligo(*p*-phenylenevinylene) derivatives formed into dimeric species first before gelation in dodecane[26]. In another Rogers' work, they carefully calculated the nucleation rate in distinct solvents under nonisothermal condition by counting the nucleus in bright-field images for 12-hydroxystearic acid gelator[21]. Much progress have been made on gelation process, and rheology method is widely used. Liu and coworkers firstly report the crystallographic mismatch theory and used the Dickinson model to analysis kinetic rheological data coupled with in-situ measurement to characterize the different fractal dimensions under different experiment condition[27-28]. Huang and coworkers investigated the isothermally gelation process of CNC and CeNC under distinct incubation temperature and establish the relationship between kinetic fractal dimension analysis and morphology of the aggregates by in-situ POM observation[12-13].

There are many factors that can influence the gelation behaviour of certain gelator thus modulate the morphology the aggregates

[a] Key Laboratory of Automobile Materials, Ministry of Education, Institute of Materials Science and Engineering, Jilin University, Changchun 130012, People's Republic of China.
[b] College of Physics, Jilin University, Changchun 130012, PR China.
* Corresponding author: E-mail: minli@mail.jlu.edu.cn Tel: +86-431-85168254
†Electronic Supplementary Information (ESI) available: See
DOI: 10.1039/x0xx00000x

Soft Matter Accepted Manuscript

further regulate the properties. Using additives is a powerful way to change the morphology of gels. It is concluded that the induction of polymeric additives lead to a significantly reduce of critical gel concentration, increase of nucleation rate and increase in gel strength[29] for pyridine-based gelators in Yash's work. Effect of solvent on the morphology of the gel is also discussed and analysed using the Hansen solubility parameters of solvent, however, how the solvents interact with gelator molecular remains unclear. Our group demonstrated the ultrasound-induced gelation for twin-tapered dihdrazide derivatives, and proposed that the main effects of ultrasound are on the non-aggregated molecules[20]. The main difficulty for the investigation on the nucleation mechanism and bundling process of fibers is the technology limit and the models used to analysis kinetic data are too idealized for the complex gel system.

In order to gain a deep understand on the crystallization nature of gelation process. Our present work investigate the effect of incubation temperature on the gels from a gelator BP8-C, a bent-core dihydrazide derivative in both $CHCl_3$ and toluene. The gels of BP8-C from $CHCl_3$ showed either transparent gels or opaque gels depending on incubation temperature, and the nucleation time decreased as the incubation temperature decreased with exponent relationship. Kinetic results showed that the *n* values of gelation BP8-C in $CHCl_3$ are varied between1.21 and 1.44 at incubation temperatures of 0 ℃to 20 ℃. Its D_f factor based on Dickinson model are between 1.36 and 1.45 at different incubation temperatures. For its gelation of toluene, nucleation time shows logarithmic relationship with incubation temperature, which is quite unusual. And BP8-C can't gel toluene below 0 ℃ though the concentration is much higher than its critical gelation concentration. The kinetic process in toluene shows a two-phrase mechanism based on the *n* values. We proposed that the nucleation process driven by supersaturation in $CHCl_3$ and governed by mass transfer in toluene. In all, our studies suggest that temperature-dependent gelation rates of BP8-C in different solvents were quite different and the properties of a gel are largely affected by the history of sols.

Experimental

Synthesis of BP8-C

The syntheses route and characterizations are included in the Supporting Information.

The compound BP8-C was synthesized according to the route shown in Scheme S1 which was similar to that of BPH-n[30] and FH-Tn[31-32]. Isophthaloyl dichloride was regularly injected into the THF solution of 3,4-dioctyloxy-benzhydrazide ($mol_{chloride}/mol_{hydrazine}$ = 1/2) with vigorous stirring at room temperature for 8 h. The crude product was isolated and further purified by recrystallization from ethanol for further ^{1}H NMR, FT-IR measurements, and elemental analysis; yield = 76%. The melt point is 204 ℃ confirmed by DSC, and the M_W is 915.25 g/mol.

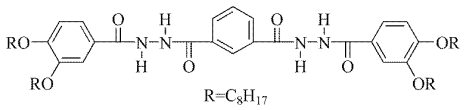

Scheme 1. Molecular structure of BP8-C.

General testing methods

All staring liquids were obtained from commercial supplies. Xerogels were prepared by freezing and pumping the organogel of BP8-C for 24 h. Field emission scanning electronic microscopy (FE-SEM) observations were recorded with a SSX-550 apparatus. X-Ray diffraction (XRD) was carried out on a Bruker Avance D8 X-ray diffractometer. Solubility studies based on 1H NMR data were collected from a Bruker Avance 500Hz using tetramethylsilane (TMS) as an internal standard (δ=0.00) and phenyl-trimethylsilicane as an internal standard. Fourier transition IR spectrum (FT-IR) measurement was carried on a Perkin-Elmer spectrometer (Spectrum One B). The xerogels were pressed into a tablet with KBr for FT-IR measurements. Photoluminescence was measured on a Perkin-Elmer LS 55 spectrometer. Differential scanning calorimetry (DSC) curve was obtained on a Netzsch DSC 204 instrument. Optical textures (POM) were observed under a Leica DMLP microscope equipped with a Leitz 350 heating stage.

Results and discussion

Preliminary Gelation Studies

To assess the gelation behavior of the gelators in a simple way, reproducible tube inversion experiments were performed[33], and BP8-C showed strong gelation ability in many organic solvents as show in Table 1. All tests were carried out at room temperature (about 20 ℃), and the concentration of the solution is 12 mg/mL. BP8-C is demonstrated to gel different alcohols, except methanol, and the m_{CGCs} is as low as 2.65 mg/mL (in 1-propanol). BP8-C shows good gel ability in benzene, chlorobenzene, toluene and $CHCl_3$ in which its m_{CGC} is 2.4 mg/mL at room temperature. In contrast, it is soluble in DMSO, DMF, pyridine and cyclohexane. While BP8-C can dissolve in THF and methanol upon heating and precipitate while cooling down, it is insoluble in acetonitrile.

It is interesting that BP8-C formed two different gels i.e. transparent gel (T-gel) and opaque gel (O-gel) in chloroform depending on the incubation temperature of the sols. The transparent gel prepared at temperatures higher than 10 ℃ showed higher stability than that of the O-gels (see photo S1), which were prepared at lower incubation temperature (lower than 5 ℃). Furthermore, the appearance of either transparent or opaque gel of BP8-C in chloroform depends only on incubation temperature, while independent on its concentrations within the scope of our attempted (as high as 50 mg/mL). In addition, the lower the incubation temperature, the faster the gelation process. In contrast, BP8-C formed only opaque gels in toluene and it took longer time to gel with the decrease of incubation temperature.

Soft Matter Accepted Manuscript

This journal is © The Royal Society of Chemistry 20xx

Please do not adjust margins

Table 1 Critical Gelator Concentration (CGCs, mg/mL) in Different solvents As Determined in 1 cm (I.d.) Tubes for BP8-C.

Liquid	BP8-C	Liquid	BP8-C
DMSO	S	acetonitrile	I
DMF	S	pyridine	S
THF	P	methanol	P
DCE	G (4.2)	ethanol	G (2.8)
$CHCl_3$	G (2.4)	1-propanol	G (2.65)
benzene	G (3.5)	1-butanol	G (2.68)
toluene	G (3.3)	1-pentanol	G (2.87)
dimethylbenzene	G^P	1-hexanol	G (2.48)
chlorobenzene	G^T (2.14)	1-octanol	G (2.72)
cyclohexane	S	1-decanol	G (2.93)

S = solution, P = precipitate, I = insoluble, G^P = partial gel, G^T = transparent gel. The concentration of the solutions is 12 mg/mL.

And no gelation was observed at lower incubation temperatures (below 0 ℃) and at last precipitate in a few days although the concentration we have tried is 50 mg/mL. Fig.1 shows the gel–sol transition temperature (Tg, based on tube inversion measurements, reflecting the breakdown of the samples panning network) of T-gel, O-gel and gels formed in toluene. Typically, as the molar concentration was increased, Tg increased until a plateau region is reached. The Tg of T-gel is almost 10 ℃ higher than that of O-gel at the same concentration in chloroform. And the gels formed in toluene show better thermal stability than those in $CHCl_3$ which may be due to the solubility difference based ^{1}H NMR studies.

^{1}H NMR studies on solubility

For a determinate gel system, it is considered that the gelator will incorporated into two phases, i.e. the solid-like fibrillar network and the liquid-like solution phase[34]. The gelators in solution phase can be detected by ^{1}H NMR. The concentration of gelator in liquid phase measured via integration against an internal standard, phenyl-trimethylsilicane, which is considered immobile in the liquid phase all the time. As reported, gelators that has been incorporated into the solid-like gel network exhibits broadened peaks, thus can be considered to not contribute significantly to the observed spectrum[35]. We use the ^{1}H NMR method to measure the relative concentrations of gelator in the two phases. It is worthwhile to note that measurements were carried out at concentrations above CGCs and temperatures below T_g. For an

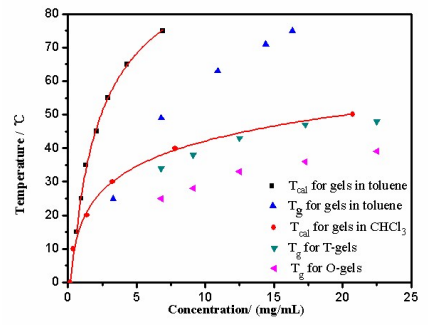

Fig. 1 The gel-sol transition temperature of BP8-C in $CHCl_3$ and toluene and the calculated T_{cal} values based on solubility values.

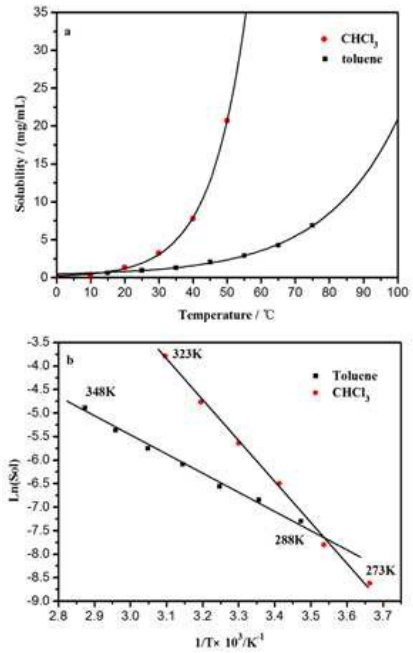

Fig.2 (a) Gelator solubility of BP8-C.Symbols represent experimental data, solid line represents predicted solubility based on the van't Hoff equation; (b) Plot of ln(*Sol*) (*Sol* = solubility, i.e., the concentration of gelator species in solution) against the reciprocal of the dissolution temperature (toluene: slope = -3.93, intercept = 6.30, R^2 = 0.991; $CHCl_3$: slope = -8.59, intercept = 22.79, R^2 = 0.996).

ideal solution system, the solubility at a given temperature can be expressed by van't Hoff equation:

$$\ln (Sol))=(-\delta H_{diss}/RT_{eq})+(\delta S_{diss}/R) \qquad (1)$$

δH_{diss} and δS_{diss} means the molar enthalpy and the molar entropy for the dissolution process (i.e., gel-sol transformation), T_{eq} is the

Soft Matter Accepted Manuscript

equilibrium temperature, and *R* is the gas constant. We used the collected data to calculate δH_{diss} and δS_{diss}, and extended the theoretical solubility at different temperatures. Fig.2a plots the effective solubility of BP8-C as observed by ^{1}H NMR spectroscopy at different temperatures (points) against the theoretical fit as predicted by the van't Hoff equation using the derived thermodynamic parameters, δH_{diss} and δS_{diss} (solid lines). The calculated δH_{diss} and δS_{diss} for BP8-C in toluene are 32.68 kJ mol^{-1} and 52.36 J mol^{-1} K^{-1} (see Fig.2b). For BP8-C in $CHCl_3$, δH_{diss} and δS_{diss} are 71.38 kJ mol^{-1} and 188.96 J mol^{-1} K^{-1}. As would be expected, increasing temperature would increase the observed solubility of the gelator in certain solvents. The gelation process and the properties of a gel would be affected by the incubation temperature.

We further develop this approach based on solubility, in order to relate the theoretical solubility data derived from the van't Hoff analysis (used in Fig.2a) to the T_g data obtained from simple gel tube inversion methodology (Fig.1). In general terms, Fig.1 demonstrates a good correlation between the theoretical thermal profiles based on solubility (solid lines) and the experimentally measured T_g data (symbols). It is noteworthy that this approach, based on gelator solubility, T_{cal} extracted from the van't Hoff equation, relating to complete solubilization of the networked gelator. However, T_g corresponds to the temperature at which the gel network is partly dissolved and the remaining sample-spanning gel network becomes unable to self-support. The T_g values are all lower than T_{cal} for T-gel and O-gel and gels formed in toluene. The deviate of T_g from T_{cal} in toluene are larger than that in $CHCl_3$, which might be associated to the low solubility thus lead to its underestimation. The solubility studies show evidence that the supersaturation will play a positive role during the gelation process of BP8-C in $CHCl_3$ and toluene.

Nucleation time and gelation rate

As mentioned above that transparent gel could be resulted if BP8-C/$CHCl_3$ sols incubated at temperatures higher than 10 ℃, otherwise the opaque gel. In addition, the lower the incubation temperature, the shorter the gelation time for the BP8-C/$CHCl_3$ sols. In contrast, BP8-C form opaque gels in toluene at temperatures higher than 0 ℃. Herein, photoluminescence method was used to evaluate the influence of the incubation temperature on nucleation and gelation of BP8-C in different solvents.

The photoluminescence spectra of the BP8-C in $CHCl_3$ at different concentrations and in its gel were shown in Fig.3a, BP8-C in hot $CHCl_3$ solution (8.6×10^{-4} mol/L) exhibited two strong fluorescence at 413 nm and 438 nm (λ_{ex} = 370 nm), which are attributed to the intramolecular π^*-π transitions, while a broad emission centered at 408 nm (λ_{ex}=339 nm) was observed in the cold solution ($CHCl_3$, 8.6×10^{-4} mol/L) suggesting that cooling resulted in aggregates of molecules. The BP8-C gel from $CHCl_3$ (at 8.6×10^{-3} mol/L) showed a further blue-shifted emission at 371nm (λ_{ex}=339 nm) compared to that of cold solution in $CHCl_3$ at 8.6×10^{-4} mol/L. It can be envisioned that this aggregation-induced blue-shifting of the

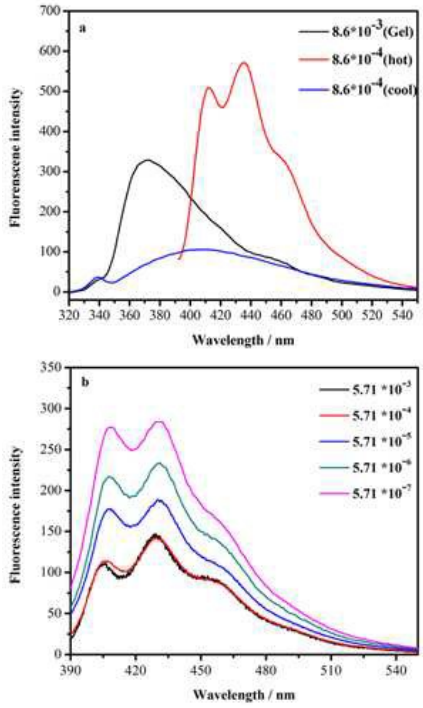

Fig.3 Fluorescence spectra of BP8-C at different concentrations (mol/L) under room temperature. (a) in $CHCl_3$; (b) in toluene (λ_{ex}=339 nm).

emission is due to the conformation transition as well as the intensity increased upon gelation (see Fig. S1) indicating the formation of J-aggregates. BP8-C showed similar aggregation behaviour in toluene. It showed emissions at λ = 408 nm and λ = 430 nm (Fig.3b) in hot toluene while shifted to λ = 360 nm (λ_{ex} = 320 nm) in the corresponding cold one, indicating conformation transition and J-aggregates form upon gelation.

Fig.4a shows the typical intensity changes (λ_{ex} = 339 nm, λ_{em} = 370 nm) of 5.00 mg/mL BP8-C in $CHCl_3$ during the gelation. It can be seen that the fluorescence emission intensity changed little with time at the early stage of gelation and it increased drastically until a plateau was reached, indicating that the fibrillation of BP8-C in $CHCl_3$ was autocatalytic and following a nucleation-crystalline mechanism. The time at which the intensity began to increase rapidly is defined as on-set point when gelation occurred (t_g), and the time at which the maximum intensity reached is considered as the accomplishment of gelation. Here we adopt polymer crystallization theory to estimate the gelation rate as $K = 1/t_{1/2}$, nucleation time (t_1) is defined as the period from t_0 to t_g and gelation time (t_2), the period from t_g to t_{max}. For BP8-C/$CHCl_3$, t_1 and t_2 increased from 172 s, 333 s at 0 ℃ to 366 s, 682 s at 20 ℃, and the gelation rate $K = 1/t_{1/2}$ decreased from 6.17 × 10^{-3} s^{-1} at 0 ℃ to 3.00 × 10^{-3} s^{-1} 20 ℃. Thus lower incubation temperature could accelerate the gelation of BP8-C in $CHCl_3$ as shown in Fig. 3a. Both gelation time and galation rate of BP8-C in toluene showed

Soft Matter Accepted Manuscript

This journal is © The Royal Society of Chemistry 20xx

Please do not adjust margins

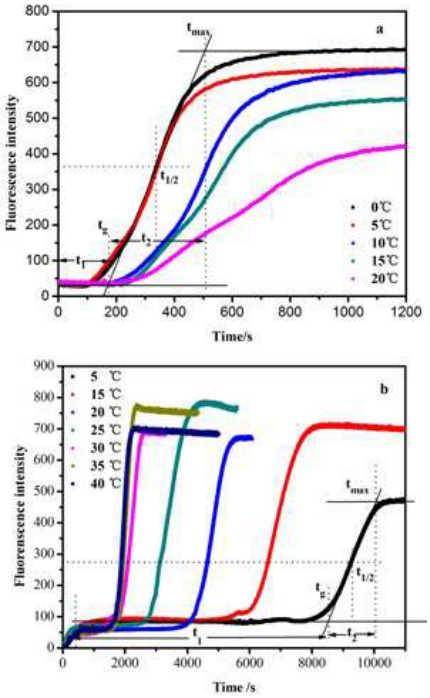

Fig.4 (a) Dynamic fluorescence intensity for a 5.00 mg/mL BP8-C/$CHCl_3$ sample undergoing gelation process; (b) Dynamic fluorescence intensity for a 5.34 mg/mL BP8-C/toluene sample (partial gels at 40 ℃).

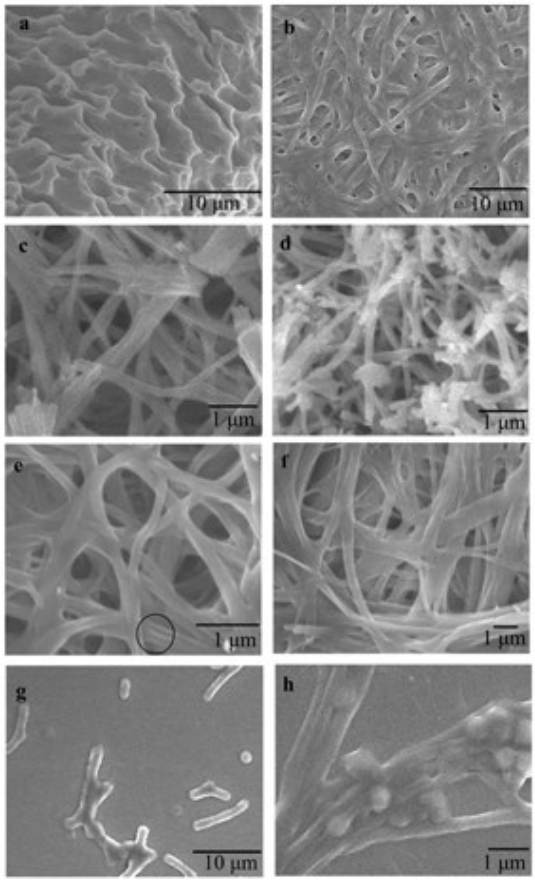

Fig.5 SEM pictures of xerogels from $CHCl_3$ and toluene, (a) T-gels incubated under 20 ℃; (b) O-gels incubated under -24 ℃; (c) xerogels of 10.12 mg/mL incubated under 30 ℃; (d) xerogels of 5.34 mg/mL incubated under 30 ℃; (e) xerogels of 10.12 mg/mL incubated under 10 ℃; (f) xerogels of 5.34 mg/mL incubated under 10 ℃; (g)precipitate of 10.12 mg/mL incubated under -24 ℃; (h) precipitate of 5.34 mg/mL incubated under -24 ℃.

opposite temperature-dependent logarithmic behaviour compared to that in chloroform (see Fig. 4b). The t_1, t_2 values of BP8-C/toluene (5.34mg/mL) sols decreased from 1197 s to 7370 s at 0 ℃ and 563 s to 1246 s at 35 ℃. The t_1, t_2 values for partial gels of sols incubate at 40 ℃ are close to that incubated at 35 ℃. Meanwhile, the gelation rate increased from 1.00×10^{-3} s^{-1} at 5 ℃ to 4.10×10^{-3} s^{-1} 35 ℃. Similar temperature-dependent gelation behaviour was observed for 10.12 mg/mL BP8-C/toluene sols (see Fig.S2). And detailed values of t_1, t_2, $t_{1/2}$, *K* are given in Table.S1, Table.S2, Table.S3 for 5.00 mg/mL BP8-C/$CHCl_3$, 5.34 mg/mL BP8-C/toluene and 10.12 mg/mL BP8-C/toluene respectively. Meanwhile, t_1, t_2, $t_{1/2}$ verse incubation temperatures for 5.00 mg/mL BP8-C in $CHCl_3$ and 5.12 mg/mL in toluene are given in Fig.S3 Carefully examine the *t* values, it can be concluded that the nucleation rate is dependent on the concentration, i.e. the *K* values are 1.87×10^{-3} s^{-1} for 5.34 mg/mL and 2.40×10^{-3} s^{-1} for 10.12 mg/mL at 20 ℃, suggesting that the supersaturation is in favor of nucleation.

For the nucleation of BP8-C gelator, nucleus formed during t_1 times and once nucleus formed the fibers grow rapidly. At the same time, the growth of fibers and bundling process are sensitive to the incubation temperature. It is generally accepted that gelation process is similar to crystallization in solution. However, there is no clear mechanistic understanding of nucleation even for either polymer or inorganic salt, only some empirical results. We courageously guess that density fluctuation (supersaturation) governs the nucleation of BP8-C in $CHCl_3$ because its solubility decreased sharply as temperature decreased, while in toluene, the nucleation might be affected by both supersaturation and mass transfer (diffusion) parameter which is the driven force for nucleation because its solubility in toluene changed not too much compared to that in $CHCl_3$.

From the above analysis, it can be concluded that the the gelation process of BP8-C, e.g., galation time and gelation rate could be affected by not only solvent and concentration but also incubation temperature and it showed different temperature-dependent behaviour in different solvents.

Soft Matter Accepted Manuscript

SEM morphologies

FE-SEM images of BP8-C/$CHCl_3$ xerogels are shown in Fig.5. It shows that networks of T-gel in chlorofrom (Fig.5(a)) are more trammel-like, which is a more stable structure. While xerogels of the O-gel (Fig.5(b)) consist of fibers with the width about 1μm, which are entangled to form networks to sustain solvent therein. The formation of fibers indicates they are driven by strong directional intermolecular interactions. BP8-C showed different morphologies in toluene depending on the incubation temperature and the concentration. The BP8-C xerogels prepared at 30 ℃, from 10.12 mg/mL toluene (Fig.5(c)) showed tangled fibers which are short with 180 nm in width while for the sols of 5.34 mg/mL, uniformly belt-like fibers about 200 nm in width were observed in Fig.5(d). When incubation temperature is lower to 10 ℃, thin fibers of 100 nm in width are bundling into fasciculus and the fiber are inclined to twine together as shown in Fig.5(e) of 10.12mg/mL, thin fibers bundled into fasciculus about 1.5 μm in width were observed for the xerogels prepared at 5.34 mg/mL (Fig.5(f)). Precipitates of BP8-C in toluene (10.12 mg/mL) prepared at -24 ℃ (Fig.5(g)) showed both short sticks with 2 μm in width and about 10 μm of average length, and sphere-like particles with diameter about 0.5 μm. While precipitate prepared from the 5.34 mg/mL sols cooled rapidly to –24 ℃ showed the coexistence of spheres (ca.1 μm in diameter) and fibers (Fig.5(h)),which are constructed by the particles. In all, the compact trammel-like networks for BP8-C/$CHCl_3$ T-gels give rise to a more stable one than fibers tangled networks of O-gels. While BP8-C from toluene showed different morphologies depending on the incubation temperature regardless the concentration, fibers constructed networks for gels and short sticks as well as sphere-like particles for precipitate.

Molecular arrangement

To illustrate the molecular arrangement of the gels or the precipitates at different incubation temperatures, wide angle X-ray diffraction (XRD) measurements were performed. As shown in Fig.6(a), the XRD paterns of the xerogels prepared from $CHCl_3$ show similar series of reflections. In each series, the various *d*-spacings observed form a suite of fractions (*d*/1:*d*/√3:*d*/2), a feature that strongly suggests a hexagonal columnar structure[36]. The incubation temperature influences the *d*-spacing to a small but significant extent. The *d*-spacing values are 30.05 (100), 17.32 (110), 15.02 (200) for T-gel (*a* = 34.70 Å), and 29.25 (100), 16.86 (110), 14.63 (200) for O-gel (*a* = 33.77 Å), respectively. And the diffuse reflection at 2θ = 21° was ascribed to the aggregation of alkyl chains, and peaks at 2θ = 6.48°, 6.25° means the order of the chains. The XRD patterns (Fig.S4) of the xerogels or precipitant extracted from BP8-C/toluene gels incubated at different temperatures all show a hexagonal columnar structure with *a* = 35.90 Å, although they were prepared at different temperatures or different concentrations. The molecular packing of BP8-C either in xerogels from $CHCl_3$ or those from toluene showed almost the same Col_h pattern, and the slightly difference in lattice parameter *a* can be explained as solvent molecules penetrate within the

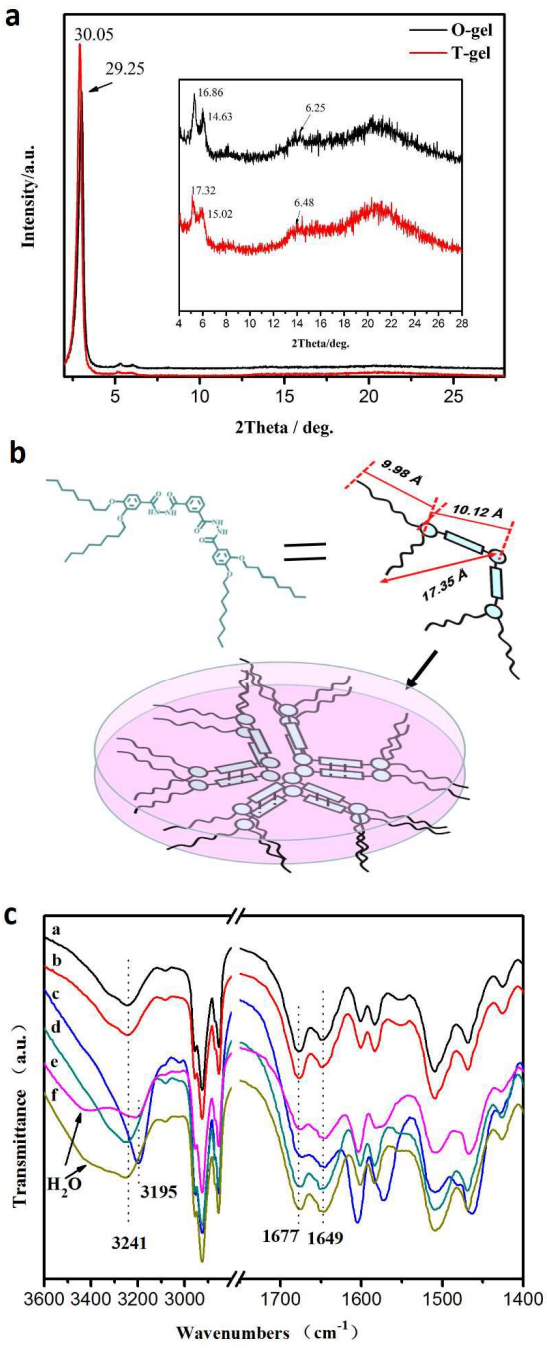

Fig.6 (a) XRD results of xerogels from BP8-C/$CHCl_3$ with the concentration of 5.00 mg/mL. (b) Packing model for BP8-C. (c) Partial FT-IR spectra of BP8-C: (a) xerogels of T-gel in $CHCl_3$, 20 ℃, 5.00 mg/mL; (b) xerogels of O-gel in $CHCl_3$, -24 ℃, 5.00 mg/mL; (c) xerogels from toluene, 20 ℃, 10.12 mg/mL; (d) precipitant from toluene, -24 ℃, 10.12 mg/mL; (e) xerogels from toluene, 20 ℃, 5.34 mg/mL; (f) precipitant from toluene, -24 ℃, 5.34 mg/mL.

Soft Matter Accepted Manuscript

This journal is © The Royal Society of Chemistry 20xx

aggregates. The average number of molecules (μ) in a column slice can be calculated through the equation $\mu = (\sqrt{3}\, N_A \cdot a^2 \cdot h \cdot \rho)/2M$ for the hexagonal phase, where N_A is Avogadro's number, a is the lattice constant, h is the intracolumnar periodicity (h = 0.42 nm), ρ is the density (assumed to be 1 g/cm^3), and M is the molecular weight of the compound. The calculated average number of molecules in each slice of column was 3.08 for xerogel from toluene and 2.88 for T-gel. The calculated lengths of the rigid part and the terminal flexible chain assuming that the -CH_2- groups are in all-trans conformation are 10.12 Å and 9.98 Å, respectively (Figure 6b). Combining the results of XRD and the calculated molecular size of BP8-C, the schematic molecular arrangement within one column of the xerogels of BP8-C was given in Figure 6b. We proposed that molecules self-assembled through intermolecular hydrogen boning along the axis of the columns and approximately three gelators formed a trimmer-like structure in each columnar slice, canceling the dipole repulsions between the molecules and diminishing the polarities of the molecules.

FT-IR spectroscopy gives direct information about the hydrogen bond interactions. FT-IR spectra of the xerogels from $CHCl_3$ are identical (Fig.6 (c)) in spite of the SEM results are obviously different, suggesting that the incubation of the sols influenced the gelation process but not the nucleation of nanometer scale. The N-H stretching bands emerge at 3241 cm^{-1} and two strong C=O stretching bands at 1649 cm^{-1}, 1677 cm^{-1} for $CHCl_3$ xerogels, which suggests the hydrogen bond is formed between -N-H and -C=O[37-38]. Meanwhile, for BP8-C/toluene xerogels or precipitant N-H stretching bands located at 3195 cm^{-1} incubated under 20 ℃ at concentrations of 10.12 mg/mL and 5.34 mg/mL, which shifted to 3241 cm^{-1} while incubated at -24 ℃. The -C=O stretching bands located at 1677 and 1649 cm^{-1}. Low wavenumbers of N-H stretching bands as well as -C=O indicated strong hydrogen bond between -N-H and -C=O interactions. Detail data of the FT-IR results are given in SI.

Kinetic Studies Based on Dickinson Model and Avrami Model

Analysis of the fractal nature of our molecular organogels is based upon a kinetic model which was first proposed for dilute system developed by Dickinson[39] (eq.2) and Avrami model (eq.3 and eq.4) which were initially used to describe the crystallization of polymer melts[40-41] to measure the fractal structure of nanostructure networks during gelation process. Herein, we analyst our kinetic data using these two models in order to simulate the gelation process of BP8-C in different solvents and at different incubation temperatures. The fractal dimension parameter D_f indicates the growth mode of the fiber network and the Avrami parameter n provide information about the shape of the objects formed and their mechanism of nucleation which related to the interaction of the fibers. In our fluorescence method, the excluded volume of the aggregate ($X_{(t)}$) is related to the fluorescence intensity.

$$\ln\frac{X_{(t)}-X_{(0)}}{X_{(\infty)}-X_{(0)}} = C + (3-D_f)/D_f \ln t \qquad (2)$$

$$\ln\left[1-X_{(t)}\right] = -kt^n \qquad (3)$$

$$\ln[-\ln\frac{X_{(\infty)}-X_{(t)}}{X_{(\infty)}-X_{(0)}}] = n\ln k + n\ln t \qquad (4)$$

where t is time, k is a temperature-dependent parameter like a rate constant, D_f is the fractal dimension, n is the Avrami parameter indicating the degree of branching and fiber-fiber interaction[15]. $X_{(t)}$ is the volume fraction of the gel phase at time t, expressed fluorescence intensity at time = 0, t, and ∞ ($X_{(0)}$, $X_{(t)}$, *and* $X_{(\infty)}$) in the present study, zero-time is defined as fluorescence intensity starts to increase rapidly.

Fig.7 shows Avrami plots and Dickinson plots based on kinetic fluorescence data of BP8-C/$CHCl_3$ gels (5.00 mg/mL) prepared at different incubation temperatures. Obviously, the T-gels showed a larger Avrami parameter (n) than that of the O-gels. Values of n jumped from 1.21 to 1.44 for gelation at temperatures 0 to 20 ℃. This jump of n indicated that fiber-fiber interactions are more compact in gels formed at higher incubation temperature (20 ℃). However, the D_f values undulate between 1.45 and 1.36, suggesting a linear growth mechanism. These observations add evidence to our deduce that the BP8-C molecules in chloroform

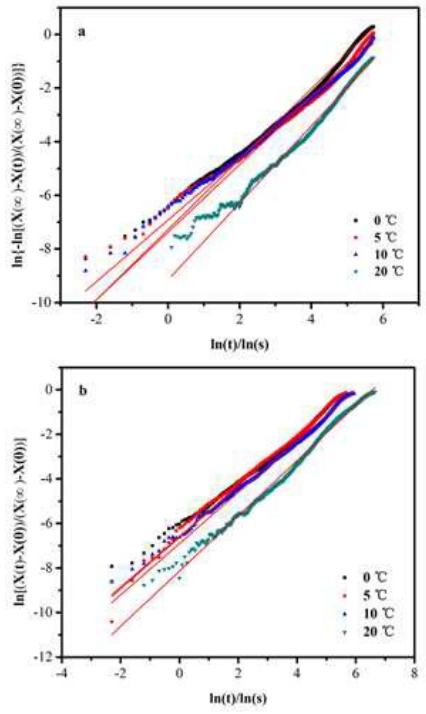

Fig.7 Kinetic plots for gelation of sols of 5.00 mg/mL BP8-C/$CHCl_3$. (a) Avrami data (0 ℃, n = 1.21, R^2 = 0.986), (5 ℃, n = 1.26, R^2 = 0.978), (10 ℃, n = 1.31, R^2 = 0.992), (20 ℃, n = 1.44, R^2 = 0.988). (b) Dickinson data (0 ℃, slope = 1.14, D_f = 1.4, R^2 = 0.993), (5 ℃, slope = 1.16, D_f = 1.39, R^2 = 0.993), (10 ℃, slope = 1.15, D_f = 1.39, R^2 = 0.994), (20 ℃, slope = 1.21, D_f = 1.36, R^2 = 0.991).

Soft Matter Accepted Manuscript

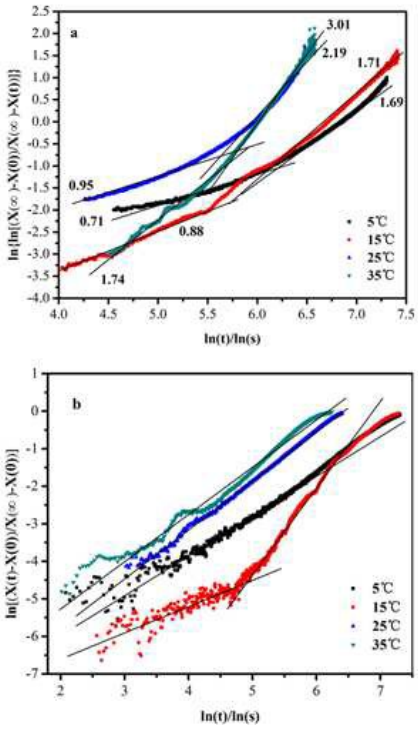

Fig.8 Kinetic plots for gelation of sols of 5.34 mg/mL BP8-C/toluene. (a) Avrami data; (b) Dickinson plots, (5 ℃, slope = 1.15, D_f = 1.39, R^2 = 0.990), (15 ℃, first stage: slope = 0.62, D_f = 1.85; second stage: slope = 1.69, D_f = 1.12), (25 ℃, slope = 1.31, D_f = 1.30, R^2 = 0.998), (35 ℃, slope = 1.26, D_f = 1.32, R^2 = 0.985).

prefer to growth 1D mechanism and fiber-fiber interaction becomes stronger at higher temperature (20 ℃), which give rises to the higher thermal stability. It can be concluded based on the above analysis on the gelation dynamics of BP8-C in chloroform that the changes of incubation temperature does not influence the nucleation mechanism which is in accordance with that of the XRD results.

Kinetic plots from Avrami and Dickinson model for BP8-C with 5.34 mg/mL BP8-C in toluene are shown in Fig.8. Obviously, Avrami based kinetic analyses of dynamic fluorescence data revealed a two-phrase kinetic process[19], featured by n = 0.88 and followed by n = 1.71 for 15 ℃, this two-phrase kinetics can be understood as : the 1D fiber growth occurred first at the gelation stage and then followed by bundling induced by the fiber-fiber interactions. n values for other incubation temperatures show similar laws. D_f values changed slightly from 1.39 at 5 ℃ to 1.30 at 25 ℃, except that D_f showing two values which are 0.62 and 1.85 at 15 ℃ and we can't explain it because of the limits of our knowledge so far. But we prefer to consider this conclusion derives from deviation of the growth rate approximation at the early stage. For gelation of 10.12 mg/mL BP8-C in toluene, the Avrami and Dickinson plots are given in Fig.S5. The Avrami data also revealed a two-phrase kinetic process similar to that in 5.34 mg/mL system, on the first stage n values were in the range of 0.74 at 10 ℃ and 0.82 at 30 ℃ followed by changes from 1.62 to 1.57 at the second stage indicating that the fibers formed first and then bundling to produce compact networks. And D_f from Dickinson plots also showed a two-phrase kinetic mechanism varied between 1.87 and 1.91 followed by 1.36 at the second stage, we intend to propose that the second stage as the primary formed nucleus further aggregate into fibers as demonstrated by SEM results (see Fig.S7). Worth to note that Avrami-based kinetic analyses under incubation of 20 ℃ are unaccountable for the first stage, yet the D_f plots are in accordance with those at other temperatures. We further compare the n values of same incubation temperature with differ concentration. The slightly difference between n values reflect the less compact networks in higher concentration system as can be proved by SEM pictures shown in Fig.6a and Fig.6b at 30 ℃.

The information provided here give further demonstrates the importance of controlling the history of molecular gels. The type of solvent, concentration and incubation temperature influenced the gelation process, morphology as well as the properties of the gels. While gels prepared at different conditions showed the same molecular arrangement.

Conclusion

A new bent-core dihydrazide derivative BP8-C was designed and synthesized. BP8-C is an effective gelator which can gel most organic solvents. Interestingly, BP8-C gelled chloroform to give transparent gel (T-gel) and opaque gel (O-gel), and the T-gel prepared at 20 ℃are more thermally stable than O-gel. In contrast, opaque gel was obtained for BP8-C in toluene and it took longer time for gelation at lower incubation temperature, and precipitated below 0 ℃. By ^{1}H NMR method, the solubility of BP8-C in both $CHCl_3$ and toluene was measured and it was demonstrated that the solubility played dominant role in gelation of CHC_3 and diffusion process dominate the gelation in toluene. Although the morphology of aggregates are quite different, the molecular arrangement of gelator is all the same as Col_h with three molecules in each columnar slice. Kinetic analysis reveals the importance of the history for sols to transform into gels. It was proposed that the nucleation rate depended on supersaturation in $CHCl_3$ while on diffusion process in toluene thus the relationship between nucleation time and temperature are on the contrary. In addition, the kinetic mechanism of gelation of BP8-C in different solvents at different incubation temperatures was analyzed.

Acknowledgements

This work was supported by National Science Foundation of China (Project no. 51103057, 51073071, and 21072076) and Project 985-Automotive Engineering of Jilin University for financial support of this work.

Soft Matter Accepted Manuscript

This journal is © The Royal Society of Chemistry 20xx

Supporting Information

The synthesis routine for BP8-C and kinetic data for 10.12 mg/mL BP8-C in toluene are list in SI. BP8-C also shows liquid crystal behaviours and detail results are given in SI.

Notes and references

1. R. G. Weiss, *J. Am. Chem. Soc.,* 2014, 136, 7519.
2. L.-A. Estroff and A.D. Hamilton, *Chem. Rev.*, 2004, 104, 1201.
3. M.George and R.G. Weiss, *A cc. Chem. Res.*, 2006, 39, 489.
4. P. Terech and R. G. Weiss, *Chem. Rev.*, 1997, 97, 3133.
5. M. Lusar and C. Sanchez, *Chem. Mater.*, 2008, 20, 782.
6. N. M. Sangeetha and U. Maitra, *Chem. Soc. Rev.*, 2005, 34, 821.
7. A. Raghavanpillai, S. Reinartz and K.W. Hutcheson, *Journal of Fluorine Chemistry*, 2009, 130, 410-417.
8. Y. F. Zhou, T. Yi, T. C. Li, Z. G. Zhou, F. Y. Li, W. Huang and C. H. Huang, *Chem. Mater.,* 2006, 18, 2974.
9. J. C. Wu, T. Yi, T. M. Shu, M. X. Yu, Z. G. Zhou, M. Xu, Y. F. Zhou, H. J. Zhang, J. T. Han, F. Y. Li and C. H. Huang, *Chem. Int. Ed.*, 2008, 47, 1063.
10. M. Yamanaka, K. Sada, M. Miyata, K. Hanabusa and K. Nakano, *Chem. Commun.*, 2006, 21, 2248.
11. Z. Xu, J. Peng, N. Yan, H. Yu, S. Zhang, K. Liu and Y. Fang, *Soft Matter*, 2013, 9, 1091.
12. X. Huang, P. Terech, S. R. Raghavan and R.G. Weiss, *J. Am Chem. Soc.,* 2005, 127, 4336.
13. X. Huang, S. R. Raghavan, P. Terech and R. G. Weiss, *J. Am. Chem. Soc.,* 2006, 128, 15341.
14. Y. Liu, R. Y. Wang, J. L. Li, B. Yuan, M. Han, P. Wang and X. Y. Liu, *CrystEngComm*, 2014, 16, 5402.
15. J. Y. Xiong, X. Y. Liu, J. L. Li and M. W. Vallon, *J. Phys. Chem. B* 2007, 111, 5558.
16. X. Z. Luo, W. G. Miao, S. Wu and Y. Q. Liang, *Langmuir*, 2002, 18, 9611.
17. S. A. Ahmed, X. Sallenave, F. Fages, G. MiedenGundert, W. M. Muller, U. Muller, P. Vogtle and J.-L. Pozzo, *Langmuir*, 2002, 18, 7096.
18. N. Komiya, T. Muraoka, M. Iida, M. Miyanaga, K. Akahashi and T. Naota, *J. Am. Chem. Soc.*, 2011, 133, 16054.
19. M. M. Zhang, L. Y. Meng, X. H. Cao, M. J. Jiang and T. Yi, *Soft Matter*, 2012, 8, 4494.
20. Y. Zhang, H. Ding, Y. Wu, C. X. Zhang, B. L. Bai, H. T. Wang and M. Li, *Soft Matter*, 2014, 10, 8838.
21. M. A. Rogers and A. G. *Langmuir,* 2009, 25(15), 8556.
22. G. Y. Zhu and J. S. Dordick, *Chem. Mater.,* 2006, 18, 5988.
23. X. F. Wang and M. H. Liu, *Chem. Eur. J.,* 2014, 20, 10110.
24. J. Chen, B. Sarma, M. B. Evans and S. Myerson, *Cryst. Growth Des.* 2011, 11, 887.
25. O. Galkin, K. Chen, R. L. Nagel, R. E.; Hirsch and P.G. Vekilov, *Natl. Acad. Sci. U.S.A.* 2002, 99 (13), 8479.
26. P. Jonkheijm, P. Schoot, P. Schenning and E. W. Meijer, *Science*, 2006, July 7,313, 80.
27. X. Y. Liu and D. Sawant, *Appl. Phys. Lett*. 2001, 79(21), 3518.
28. X. Y. Liu and D. Sawant, *Adv. Mater.* 2002, 14, No. 6, March 18, 421.
29. J. Adhia, H. Schloemer, T. Perez and J. MeNeil, *Soft Matter*, 2012, 8, 430.
30. P. Zhang, H. T. Wang, H. M. Liu and M. Li, *Langmuir*, 2010, 26, 10183.
31. S. N. Qu, F. Li, H. T. Wang, B. Bai, C. Xu, L. Zhao, B. H. Long and M. Li, *Chem. Mater.*, 2007, 19, 4839.
32. S. N. Qu, H. T. Wang, Z. X. Yu, B. L. Bai and M. Li, *New J. Chem*., 2008, 32, 2023.
33. J. E. Eldridge and J. D. Ferry, *J. Phys. Chem.*, 1954, 58, 992.
34. A. R. Hirst, I. A. Coates and D. K. Smith, *J. Am. Chem. Soc.* 2008, 130, 9113.
35. B. Escuder, M. Llusar and J. F. Miravet, *J. Org. Chem.,* 2006, 71, 7747.
36. S. Laschat, A. Baro, N. Steinke, F. Giesselmann, C. Hägele, G. Scalia, R. Judele, E. Kapatsina, S. Sauer, A. Schreivogel and M. Tosoni, *Angew. Chem. Int . Ed.*, 2007, 46, 4832.
37. D. M. Pang, H. T. Wang and M. Li, *Tetrahedron* 2005, 61, 6108.
38. H. T. Wang, B. L. Bai, F.-Q. Bai, D. M. Pang, X. Ran, C. X. Zhao, H.-X. Zhang and M. Li, *Liquid Crystals*, 2011, June, Vol. 38, No. 6, 767.
39. E. Dickinson, *J. Chem. Soc.*, *Faraday Trans.*, 1997, 93(1), 111.
40. M. Avrami, *Journal of chemical physics*, 1939, 7, 1103.
41. M. Avrami, *Journal of chemical physics,* 1940, 8, 212.

Soft Matter Accepted Manuscript

Table of Contents Graphic

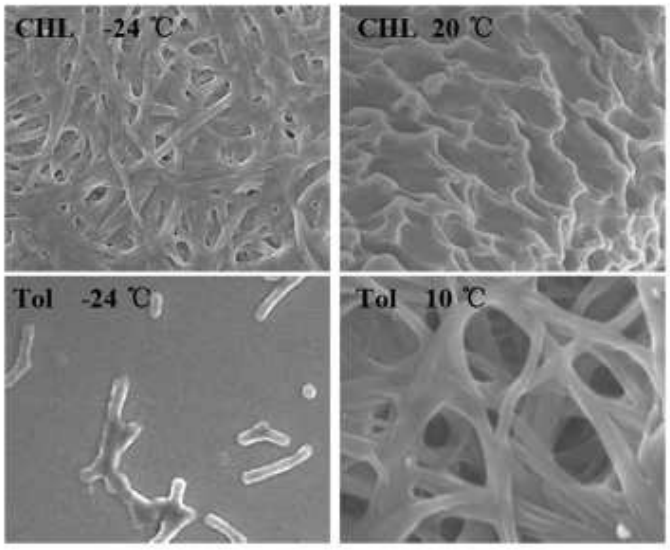

Both transparent gel and opaque gel were obtained induced by incubation temperature for sols of BP8-C in chloroform and the transparent gel formed under higher incubation temperature are more stable than opaque gel, however, gelators precipitated below 0 ℃ and form into gels under higher temperature in toluene.

Soft Matter Accepted Manuscript

This journal is © The Royal Society of Chemistry 20xx